Growth of epitaxial and polycrystalline thin films of the electron doped system $La_{1-x}Ce_xMnO_3$ through pulsed laser deposition

C. Mitra,[a] P. Raychaudhuri, J. John, S. K. Dhar, A. K. Nigam, and R. Pinto
Department of Condensed Matter Physics and Material Science, Tata Institute of Fundamental Research, Homi Bhabha Road, Colaba, Mumbai 400 005, India

(Received 27 March 2000; accepted for publication 17 October 2000)

The polycrystalline $La_{1-x}Ce_xMnO_3$ manganites do not exist in single phase in bulk under the preparation conditions so far employed, but their polycrystalline and epitaxial films deposited by the pulsed laser deposition (PLD) technique form readily in single phase. The cerium oxide (CeO_2) remains partially unreacted when the bulk sample is prepared through the solid state reaction route. The resistivity of the bulk $La_{0.7}Ce_{0.3}MnO_3$ sample shows a broad metal insulator transition (MIT) clearly resolved into two peaks, suggesting the presence of a second (impurity) phase, which is identified as unreacted CeO_2 by the intensity analysis of the x-ray diffraction (XRD) data. However, when prepared as thin films by PLD, $La_{0.7}Ce_{0.3}MnO_3$ forms in single phase, as corroborated by the uniqueness and sharpness of the MIT peak and also by the XRD patterns of the polycrystalline films. We also performed a detailed study of the epitaxial films by a high-resolution XRD system with a four-circle goniometer and did not find any impurity phase. The magnetization data shows a very sharp transition followed by a sharp MIT in resistivity at the same temperature in the epitaxial thin film. These results suggest that PLD can be used as a useful technique to synthesize unconventional compounds, which do not form easily in bulk. © *2001 American Institute of Physics.*
[DOI: 10.1063/1.1331648]

I. INTRODUCTION

In the 1950s the perovskite compounds $R_{1-x}A_xMnO_3$ (where R is a rare earth ion and A is a divalent alkaline earth metal) were extensively studied due to their remarkable magnetic behavior.[1–16] In the parent compound $RMnO_3$, which is a charge transfer insulator, the Mn^{3+} moments form a layered antiferromagnetic structure due to the superexchange antiferromagnetic interaction between the Mn^{3+} ions mediated via the intervening oxygen p orbital. The electronic configuration of Mn^{3+} is $t_{2g}^3e_g^1$, where the three t_{2g} electrons are tightly bound forming a narrow band corresponding to a localized moment with a net spin of 3/2. The electrons in the e_g orbital have a strong hybridization with the $2p$ state of a neighboring oxygen ion, and can be localized or itinerant depending on the local spin orientation[17] and carrier density. When the material is hole-doped by replacing R^{3+} ions partly by A^{2+} ions, the charge state of some Mn ions change to Mn^{4+} and the Mn^{3+}/Mn^{4+} ratio is determined by the doping level. In the doped materials the hopping of the e_g electron between spin aligned Mn^{3+} and Mn^{4+} ions gives rise to Zener double exchange interaction[4] which results in an effective ferromagnetic interaction between the Mn^{3+} and Mn^{4+} ions due to the strong on-site Hund's coupling. The strong spin-charge coupling via double exchange results in the transport and magnetic properties being correlated in these materials, and is responsible for the ferromagnetism and the associated metallic conductivity in the doped compounds. For low doping the ferromagnetic ordering temperature (T_c) of the hole doped compounds $La_{1-x}Ca_xMnO_3$ increases with doping. The 30% doped compound $La_{0.7}Ca_{0.3}MnO_3$ shows the highest ferromagnetic ordering temperature (T_c) and an associated metal insulator transition (MIT) temperature (T_p). It also has the highest negative colossal magnetoresistance (CMR) close to T_c. Near T_c, CMR occurs due to the alignment of Mn^{3+}/Mn^{4+} spins by applied magnetic field, thereby increasing the hopping probability owing to double exchange, which in turn increases the metallic conductivity.

However, Millis *et al.*[18] have shown that double exchange mechanism alone cannot explain all aspects of CMR effect, particularly the large anomalous value of resistivity above the transition temperature. The authors suggest that a polaron effect due to a strong electron–phonon coupling arising from the Jahn–Teller distortion of the Mn^{3+} ions is a necessary component for explaining the details of resistivity versus temperature curve above T_c, and the transition from a paramagnetic insulator to a ferromagnetic metal occurring at temperatures just below T_c. It may be noted that while Mn^{3+} is a Jahn–Teller ion, Mn^{4+} and Mn^{2+} are both non Jahn–Teller ions. Therefore analogous to the hole doped $La_{1-x}Ca_xMnO_3$ samples one could also have double exchange between Mn^{3+} and Mn^{2+} giving rise to ferromagnetism accompanied by MIT in the case of electron doped samples, where we partially replace Mn^{3+} by Mn^{2+} ions. In an earlier work we have shown that the layered perovskite manganites of the type $La_{1.8}Ca_{1.2}Mn_2O_7$ one can indeed obtain an electron doped system in the compounds $La_{1.8}Y_{0.5}Ca_{0.7}Mn_2O_7$,[19,20] and that the observed ferromagnetism and MIT is due to the double exchange between Mn^{3+} and Mn^{2+}. Simultaneously, Mandal and Das[21] have shown that the trivalent ion La^{3+} in $LaMnO_3$ can be partially

[a]Electronic mail: chiranji@tifr.res.in

substituted by the Ce ion, which exists in the tetravalent (Ce^{4+}) state, thereby driving some of the Mn^{3+} ions to a Mn^{2+} state. As a result the Ce doped $LaMnO_3$ compound exhibits CMR effect via the double exchange between Mn^{2+} and Mn^{3+} ions. They have shown that the system $La_{0.7}Ce_{0.3}MnO_3$ undergoes a MIT at around 250 K, though they also observed another peak in the resistivity around 225 K. They could not explain the origin of this second peak which was relatively broad compared to the first one. Subsequently, Gebhardt *et al.*[22] have reported that $La_{0.7}Ce_{0.3}MnO_3$ shows a ferromagnetic transition at around 250 K, thus confirming that the observed MIT around 250 K in $La_{0.7}Ce_{0.3}MnO_3$ is indeed due to the ferromagnetic transition, arising from double exchange between Mn^{3+} and Mn^{2+} ions. Gebhardt *et al.*[22] also observed two peaks in resistivity one at 250 K and another around 225 K, and they also did not explain the origin of the second peak. In addition to this, they observed a second transition in the magnetization data, around 43 K, which they attribute to as an antiferromagnetic transition arising from unreacted MnO_2.

We have also prepared the polycrystalline bulk $La_{0.7}Ce_{0.3}MnO_3$ sample following the solid state reaction route prescribed by Mandal and Das, and characterized them by the powder x-ray diffraction (XRD) method. Our XRD pattern is similar to that reported by Mandal and Das[21] and also to the one reported by Phillip and Kutty,[23] who prepared a sample of the same composition by wet chemical route. We performed the magnetization and transport measurements of this sample and our results were similar to the ones reported by Mandal and Das[21] and Gebhardt *et al.*[22] and we too found two peaks in the resistivity versus temperature data as observed by them. But our detailed structural analysis shows that the bulk polycrystalline sample of $La_{0.7}Ce_{0.3}MnO_3$ does not exist in single phase when prepared by the solid state reaction route. In this work we have identified the impurity phase in the $La_{0.7}Ce_{0.3}MnO_3$ bulk samples to be unreacted CeO_2, which does not react with the rest of the material completely. We also report that in contrast to the bulk sample, both epitaxial and polycrystalline films of $La_{0.7}Ce_{0.3}MnO_3$ form in single phase when deposited by the laser ablation technique. We characterized the epitaxial film using a high resolution four-circle x-ray goniometer, and the polycrystalline film using powder XRD. We found that in the epitaxial film, there is a sharp and unique MIT around 250 K as suggested by the resistivity versus temperature data, and there is no second transition in the magnetization data, unlike the one obtained by Gebhardt *et al.*[22] on the bulk sample. The purpose of studying the polycrystalline film was to check whether it is the high energetic laser ablation process or the epitaxy which is responsible for the single phase formation of the films.

II. EXPERIMENT

Bulk samples of $La_{1-x}Ce_xMnO_3$ ($x=0$, 0.025, 0.05, 0.1, 0.2, and 0.3) were prepared by solid state reaction route similar to the one followed by the previous workers.[21,22] Stoichiometric proportions of La_2O_3, CeO_2, and MnO_2 with a purity of 99.9% were mixed and ground for about 2 h. The La_2O_3 powder was preheated at 1000 °C for 12 h. The samples were then calcined at 1050 °C for 15 h. The reacted powder was reground for 1 h and annealed at 1350 °C for 15 h. The samples were characterized by XRD and we found that our XRD pattern exactly matches with the ones reported earlier.[21,23] By intensity analysis (Rietveld method) of the x-ray data we found out that the sample $La_{0.7}Ce_{0.3}MnO_3$ forms in the orthorhombic Pnma structure similar to that of $La_{0.7}Ca_{0.3}MnO_3$ and that there is a presence of a second phase which we identified as unreacted CeO_2. The amount of unreacted CeO_2 is about 20 mol % of the entire sample. These impurity peaks were mistakenly indexed by Mandal and Das[21] and by Phillip and Kutty[23] as peaks belonging to some other structural form of $La_{0.7}Ce_{0.3}MnO_3$. Gebhardt *et al.*[22] have not reported the XRD data in their article.

Using these thoroughly ground and mixed polycrystalline specimens as targets, we deposited the films by pulsed laser deposition (PLD). The epitaxial films were deposited on a $LaAlO_3$ (LAO) substrate and the polycrystalline films were deposited on a polycrystalline yttrium stabilized zirconia (YSZ) substrate. The films were deposited using a KrF excimer laser in an oxygen atmosphere. The substrates ($LaAlO_3$ and YSZ) were kept between 750 °C and 760 °C at all times. The laser energy density was approximately 3 J/cm^2 with a repetition rate of 10 Hz and the laser wavelength was 248 nm. Films were grown at an oxygen pressure of 400 mTorr. After deposition the laser ablation chamber was vented with high purity oxygen and the substrate cooled down to the room temperature. The polycrystalline films were characterized using a Siemens x-ray diffractometer and the epitaxial film was studied using a Phillips (XPERT) high resolution x-ray diffractometer comprising of a four-circle goniometer. Several reflections were taken to determine the lattice parameters. The resistance and magnetoresistance were studied by the conventional dc four-probe technique. Magnetization was measured using the Quantum Design superconducting quantum interference device (SQUID) and Oxford Instruments vibrating sample magnetometer (VSM). Surface morphology was observed using a Digital Instruments atomic force microscope (AFM) operated in the contact mode.

III. RESULTS AND DISCUSSION

A. $La_{1-x}Ce_xMnO_3$ does not exist in single phase in polycrystalline form

The XRD patterns of the polycrystalline bulk samples of $La_{1-x}Ce_xMnO_3$ which were prepared by solid reaction route are shown in Fig. 1. In this figure we have also shown the XRD pattern of CeO_2 for comparison. Figure 2(a) shows the intensity analysis (Rietveld method) of the XRD pattern of the $La_{0.7}Ce_{0.3}MnO_3$ sample using FULLPROF.[24,25] Here we have fitted the data to two different phases, the first phase corresponding to $La_{0.7}Ce_{0.3}MnO_3$, space group Pnma, and the second phase to unreacted CeO_2, space group Fm3m. The vertical bars in the first row represent the reflections corresponding to $La_{0.7}Ce_{0.3}MnO_3$ and the reflections corresponding to unreacted CeO_2 are shown in the second row. Though the intensity profiles of the experimental data and

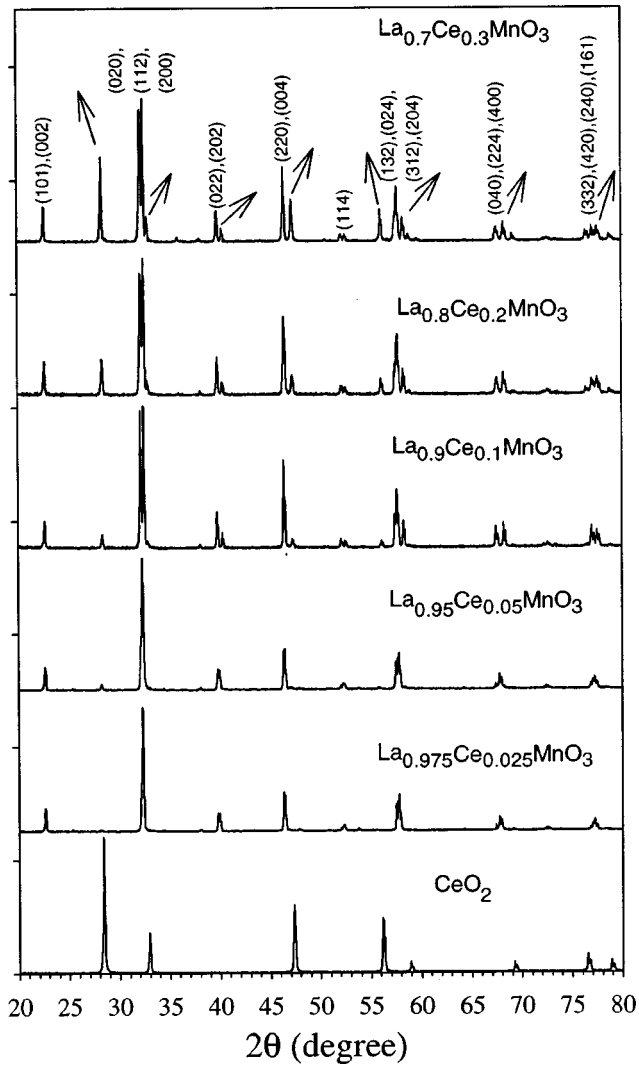

FIG. 1. X-ray diffraction (XRD) patterns of $La_{1-x}Ce_xMnO_3$ (x=0.025, 0.05, 0.1, 0.2, and 0.3) and CeO_2. The evolution of the CeO_2 peaks with increase in doping *(x)* is clearly seen. The arrows in the $La_{0.7}Ce_{0.3}MnO_3$ data indicate the presence of CeO_2 impurity peaks.

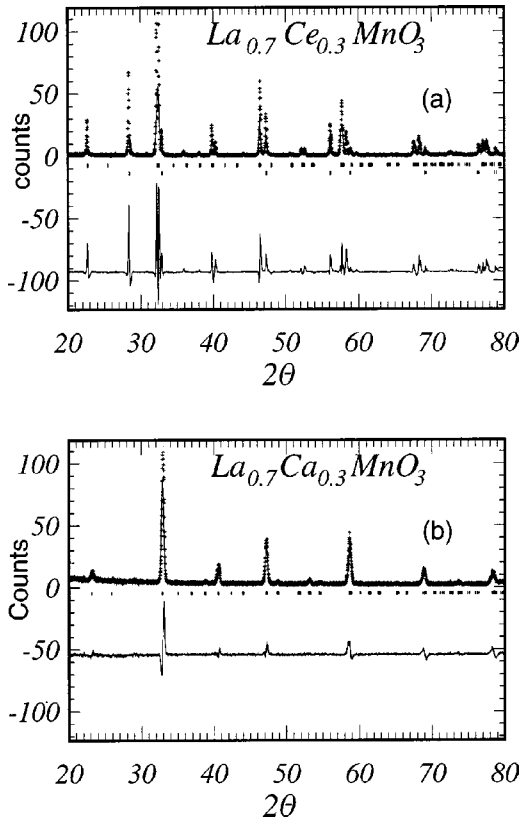

FIG. 2. (a) The x-ray diffraction pattern of $La_{0.7}Ce_{0.3}MnO_3$, with Rietveld fitting using FULLPROF. The dotted line ''+'' indicates the observed pattern, full line ''−'' indicates the calculated curve. The bottom line shows the difference between the two. The vertical bars below the fitted curve (shown as |) indicate the reflections. The vertical bars in the first line corresonds to the reflections of the $La_{0.7}Ce_{0.3-\delta}MnO_3$ phase and those in the second line represents the reflections belonging to the second phase (CeO_2). (b) The x-ray diffraction pattern (counts vs 2θ) of $La_{0.7}Ca_{0.3}MnO_3$, with Rietveld fitting. The space group to which the $La_{0.7}Ca_{0.3}MnO_3$ XRD data were fitted is Pnma.

the fitted curve do not match very well, but considering the fact that the sample contains two phases, one can conclude from our fitting the coexistence of at least 20% unreacted CeO_2 along with $La_{0.7}Ce_{0.3}MnO_3$. Gebhardt *et al.*[22] reported the presence of some unreacted MnO_2 in their sample inferred from a peak in their magnetization data around 43 K, but we did not find any signature of MnO_2 in our XRD pattern. For comparison we have also shown the fitted XRD pattern of the $La_{0.7}Ca_{0.3}MnO_3$ sample (space group Pnma) in Fig. 2(b). The XRD patterns of the bulk polycrystalline samples $La_{1-x}Ce_xMnO_3$ (Fig. 1) show an increase in the intensities of the CeO_2 peaks with the increase in doping level (x). This clearly suggests that there is unreacted CeO_2 in each sample and its concentration increases with an increase in cerium doping level.

Figure 3(a) shows the XRD pattern of the polycrystalline film of the $La_{0.7}Ce_{0.3}MnO_3$ with the sample peaks identified and labeled distinctly from the substrate (YSZ) peaks. The substrate peaks have been labeled as ''S.'' Figure 3(b) shows the XRD pattern of a blank substrate. Apparently we do not see any impurity in this XRD pattern except for a very small and broad peaklike structure around 2θ=28°, which could be due to a very small quantity of CeO_2 (less than 5%) present in this sample. The height of this impurity peak is less than 5% of that of the (121) peak of $La_{0.7}Ce_{0.3}MnO_3$, and incidentally this peak of CeO_2 has the highest intensity as is evident from Fig. 1. Using the space group Pnma, we have indexed the peaks of the XRD pattern shown in Fig. 3(a) and have calculated the lattice parameters of this sample. They are a=5.5263 Å, b=5.5025 Å, and c=7.8643 Å. The lattice parameters obtained by Rietveld refinement of the XRD pattern of the multiphase bulk polycrystalline $La_{0.7}Ce_{0.3}MnO_3$ sample are a=5.5087 Å, b=5.5431 Å, and c=7.8335 Å.

Coming to epitaxial film, we have reported earlier preliminary magnetoresistance studies of the epitaxial film of $La_{0.7}Ce_{0.3}MnO_3$ deposited on LAO substrate by the energetic PLD process. The $La_{0.7}Ce_{0.3}MnO_3$ target used for that deposition was obtained from Mandal and Das.[21] In Ref. 26, we had overlooked the fact that epitaxial films have a very sharp and unique MIT peak, as opposed to the double peak in the resistivity versus temperature curve of bulk polycrystalline sample, reported by Mandal and Das,[21] and hence we missed the fact that the bulk polycrystalline sample did not form in

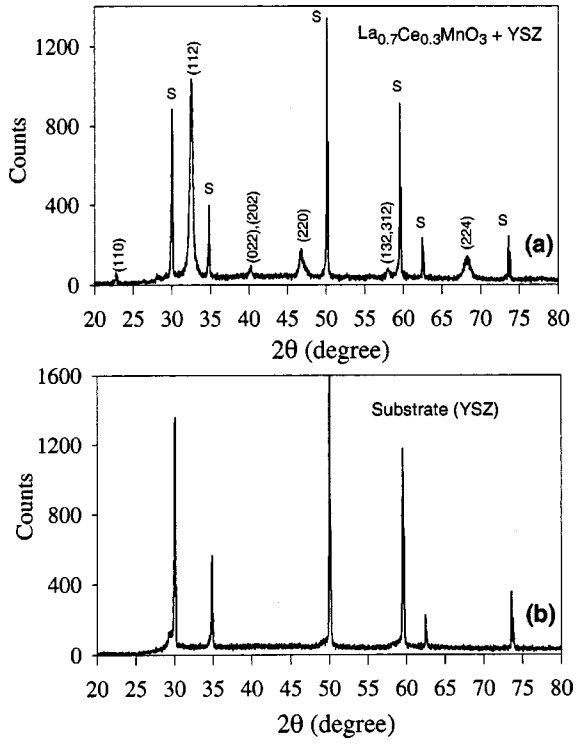

FIG. 3. (a) The XRD pattern of the $La_{0.7}Ce_{0.3}MnO_3$ polycrystalline film along with the substrate. The substrate peaks are denoted by ''S'' and the sample (film) peaks are properly indexed. (b) The XRD pattern of the polycrystalline substrate yttria stabilized zirconia (YSZ).

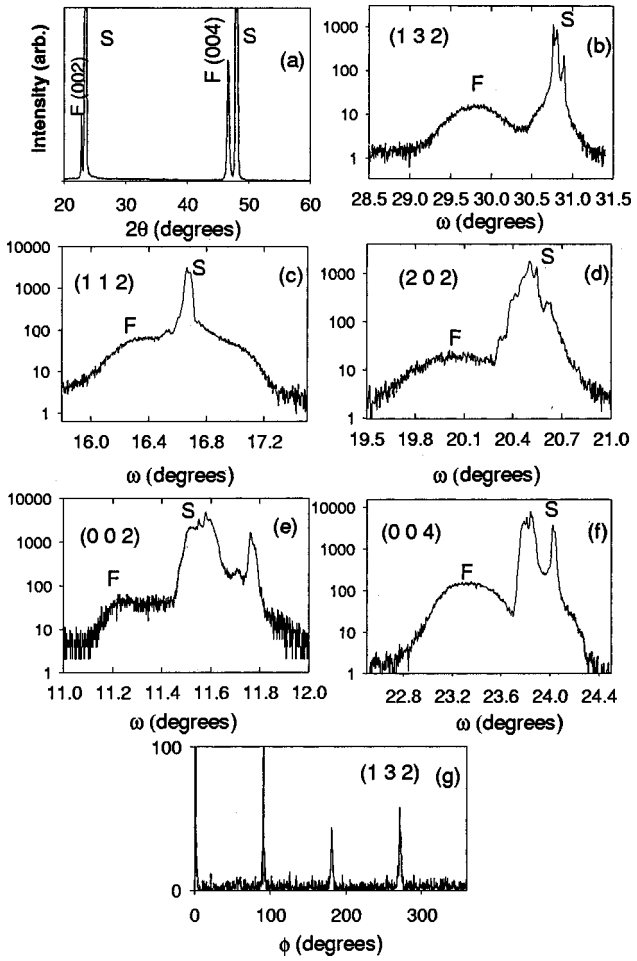

FIG. 4. (a) X-ray θ-2θ scan of the $La_{0.7}Ce_{0.3}MnO_3$ film grown at 400 mTorr oxygen pressure [thickness 3200 Å]. In this figure the substrate peaks have been labeled as ''S,'' and the film peaks have been labeled as ''F.'' (b)–(f) High resolution ω–2θ x-ray scans of different peaks of the same film. (g) ϕ-scan around the (132) peak showing the in-plane orientation (epitaxy) of the film.

single phase. The emphasis of the previous work[26] was on the magnetoresistance and how it could be enhanced by controlling the growth parameters (ambient oxygen pressure) and the thickness of the film.

In our present work we have reinvestigated the properties of the epitaxial film from a different perspective, and compared it with the polycrystalline $La_{0.7}Ce_{0.3}MnO_3$ sample. In this section the details of the characterization of the epitaxial film using x-ray diffraction is presented. The x-ray diffraction θ–2θ scans showed that the epitaxial film has an orientation $c\perp$ to the film plane. Figure 4(a) shows the representative θ–2θ scan [recorded in the Siemens x-ray diffractometer that was also used for measuring the polycrystalline samples (bulk and film)] for the $La_{0.7}Ce_{0.3}MnO_3$ epitaxial film grown at 400 mTorr showing only the (001) peaks. No impurity phase could be detected from the XRD scans in any of the films. The sample peaks are identified and labeled distinctly from the substrate (LAO) peaks. This film was also characterized by a high resolution four-circle x-ray goniometer. The lattice parameters were determined from the ω–2θ scans of five peaks, and are as follows: a=5.561 Å, b=5.512 Å, and c=7.802 Å. The ω–2θ scans of some of the peaks of the epitaxial film (thickness=3200 Å) are shown in Figs. 4(b)–4(f). The epitaxy of the films were verified from the ϕ scans around the (132) peak [Fig. 4(g)]. We could identify most of the reflections corresponding to the space group Pnma in the epitaxial sample. We did not find any impurity phase in the epitaxial film as well.

We also characterized the thin film samples using a Digital Instruments atomic force microscope (AFM) and found that the epitaxial film has well-defined grains with a grain size of about 200 nm. The AFM photographs of both epitaxial and polycrystalline thin films are shown in Fig. 5. The polycrystalline film has not so well-defined grains and there is a wide distribution of grain size with an average grain size of 75 nm, and the surface morphology is also not as good as the epitaxial film. The grains of epitaxial films were found to be larger and well-oriented because of strain effects generated by the substrate lattice, whereas the grain sizes of polycrystalline films were quite arbitrary just as expected in any polycrystalline sample. The thickness of the film reported here is approximately 3200 Å. The thickness was measured using a Dektak profilometer.

B. Resistivity and magnetization

The resistance versus temperature curve of the bulk polycrystalline $La_{0.7}Ce_{0.3}MnO_3$ sample, shown in Fig. 6(a), has two peaks, one around 250 K and another around 225 K. The peak appearing at 250 K may correspond to the MIT of the $La_{0.7}Ce_{0.3}MnO_3$ phase (which is the main phase of the two identified phases from the intensity analysis of the XRD

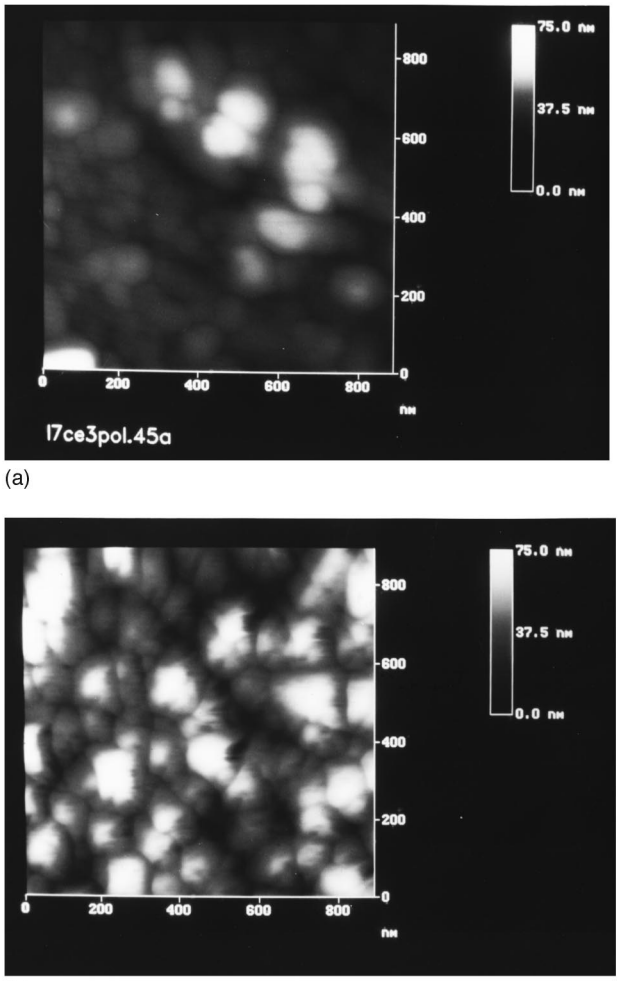

FIG. 5. (a) AFM photographs of the $La_{0.7}Ce_{0.3}MnO_3$ epitaxial thin films. (b) AFM photograph of the $La_{0.7}Ce_{0.3}MnO_3$ polycrystalline thin film.

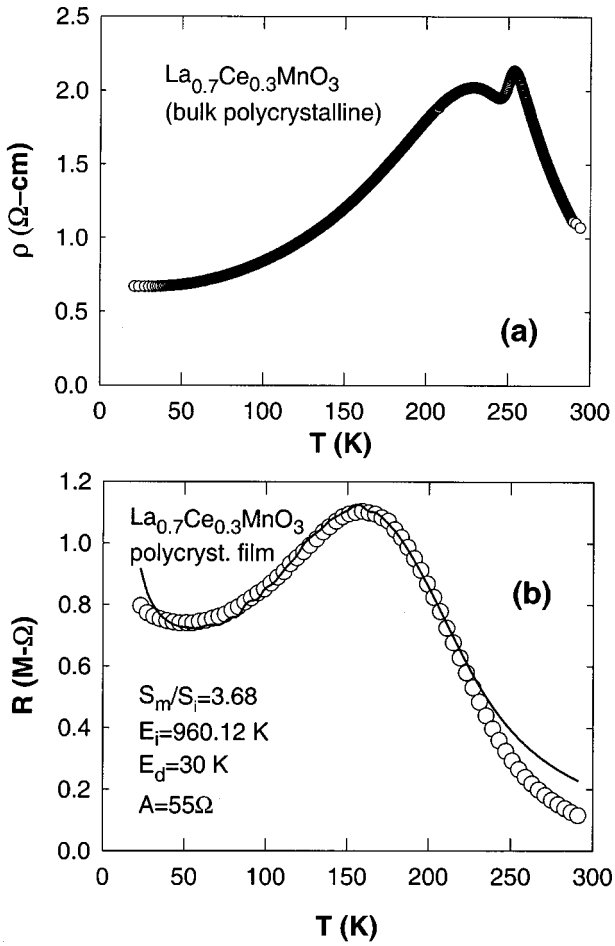

FIG. 6. (a) Resistivity vs temperature plot of the bulk polycrystalline $La_{0.7}Ce_{0.3}MnO_3$ sample. (b) The resistive vs temperature data of the $La_{0.7}Ce_{0.3}MnO_3$ polycrystalline thin film. The solid line shows the fit to Eq. (1). The fitted values of the parameter are also given in this figure.

data) and the other peak may be due to some impurity phase. But when the resistance of laser ablated $La_{0.7}Ce_{0.3}MnO_3$ epitaxial film and polycrystalline film were measured, they showed clean and unique MIT peaks as shown in Figs. 6(b) and 7(a), respectively. This corroborates our conjecture that the $La_{0.7}Ce_{0.3}MnO_3$ does not exist in single phase when prepared through the solid state reaction route, but it forms in single phase (both in polycrystalline and epitaxial films) when deposited by pulsed laser ablation.

Pulsed laser deposition has been seen to be a useful tool in many cases to stabilized unconventional crystallographic structures, as oriented, and sometimes epitaxial, films.[27] In the case of high temperature superconductors, for example, the compound $LuBa_2Cu_3O_{7-\delta}$ does not form in single phase as polycrystalline bulk, but forms in single phase as epitaxial thin films, when grown via the energetic pulsed laser deposition process. We observed that in the case of $La_{0.7}Ce_{0.3}MnO_3$ too, the material forms as single phase epitaxial thin films on single crystalline $LaAlO_3$ substrates. However, the mechanism of formation in $La_{0.7}Ce_{0.3}MnO_3$ is different from that in $LuBa_2Cu_3O_{7-\delta}$. In the case of $LuBa_2Cu_3O_{7-\delta}$ the epitaxial strain was thought to stabilize the single phase film. In our case, however, the formation of single phase polycrystalline films deposited on polycrystalline YSZ substrate by pulsed laser deposition rules out this possibility.

To understand the mechanism of formation of single phase $La_{0.7}Ce_{0.3}MnO_3$ by pulsed laser deposition one has to note that CeO_2 is an extremely stable refractory material, which does not react easily with other materials. It is therefore likely that in the solid state reaction process the CeO_2 powder is not able to react fully with the other constituents. On the other hand laser ablation is a high-energy process where bond breaking via electronic excitation and its subsequent deexcitation in the laser induced plume plays a major role, thus improving the reaction efficiency of CeO_2.

The MIT peak in the resistance versus temperature data of the polycrystalline film is considerably broad and occurs at a relatively lower temperature as compared to the epitaxial film. This is due to the fact that contribution from the grain boundaries is larger in the case of polycrystalline films compared to epitaxial films, owing to inferior surface morphology and smaller and arbitrary distribution of grain size as is evident from the AFM photographs (Fig. 5). Thus the resistance value is considerably larger here and the residual resistivity is appreciably high at the lowest temperature. In fact, the resistance tends to go up with a decrease in temperature.

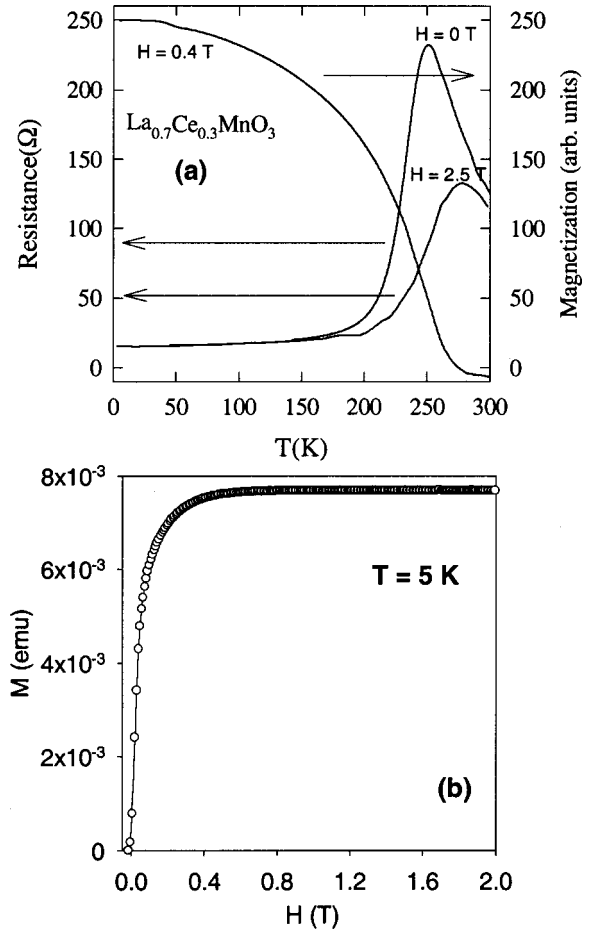

FIG. 7. (a) The magnetization *(M)* vs temperature *(T)* data of the $La_{0.7}Ce_{0.3}MnO_3$ epitaxial thin film taken at a magnetic field *(H)* of 0.4 T. Shown also are the resistance vs temperature plot of the $La_{0.7}Ce_{0.3}MnO_3$ epitaxial thin film taken at zero field and at a magnetic field of 2.5 T. (b) The *M* vs *H* data of the $La_{0.7}Ce_{0.3}MnO_3$ epitaxial thin film measured at a temperature of 5 K. Even at 2 T the *M* value has reached its saturation value, suggesting that the sample is ferromagnetic at this temperature.

One can imagine the conduction through the grain boundary to be comprised of two different conducting channels. One is through the ''pinholes'' in the grain boundary, as adjacent grains coalesce into one another at specific points, which can be considered to be good metallic regions, and the other is through the disordered region of the grain boundary, which can be considered to be an insulating barrier, with an activation energy E_i (bad-metallic regions). The situation here is similar to the one described by Andres *et al.*,[28] where the current is carried by two parallel paths: one through the pinholes in the grain boundary, which are good-metallic, and one which is bad-metallic or insulating. We fit the resistance *(R)* to an equation of the form,[28]

$$1/R=(S_m/R_m)+(S_i/R_i), \tag{1}$$

where R_m is the resistance of the pinholes and R_i is the resistance of the insulating region. S_m and S_i are, respectively, the effective sections of good-metallic and insulating (bad-metallic) channels in the polycrystalline film. The insulating barrier has a semiconductorlike resistance which is taken as $R_i \propto \exp(E_i/k_BT)$. The pinholes can be modeled as bad crystalline regions with $R_m = R_{La_{0.7}Ce_{0.3}MnO_3}$ (epitaxial film) $+A\exp(E_d/k_BT)$. The first term is the resistance of the $La_{0.7}Ce_{0.3}MnO_3$ epitaxial film. The second term accounts for strains and crystalline defects in the pinhole region. The solid line in Fig. 6(b) shows the fit to Eq. (1). The values $S_m/S_i, E_i, E_d$ and A used for the best fit of this sample are given in Fig. 6(b). Physically, S_m/S_i is the ratio of effective sections for good-metallic to the bad-metallic (insulating) conduction channels, which in this case is 3.67. The value of E_i, which gives the activation energy of the insulating barrier, is 960 K. In this scenario where the grain boundaries have an important role to play in the transport of charge carriers, the M IT temperature could go anywhere below T_c, as suggested by this fit.

The magnetization *(M)* versus temperature *(T)* data (taken at 4 kOe) of the epitaxial thin film $La_{0.7}Ce_{0.3}MnO_3$ sample is shown in Fig. 7(a) and the magnetization *(M)* versus field *(H)* data, measured at 5 K, is shown in Fig. 7(b). The latter shows that the sample is indeed ferromagnetic. Figure 7(a) also shows the resistance versus temperature data taken in zero field and at a field of 2.3 T. The resistance *(R)* versus temperature *(T)* data taken in zero field shows a unique and a very sharp MIT, suggesting the single phase nature of the film. It is clear from Fig. 7(a) that the MIT temperature (in zero field) coincides with the ferromagnetic ordering temperature (T_c). The MIT temperature is elevated by application of field and the resistance decreases, thus exhibiting a large magnetoresistance.

One final point to note is the possible band structure and the nature of ferromagnetism in the $La_{1-x}Ce_xMnO_3$ system. In perovskite manganites the e_g band gets split due to Jahn–Teller distortion into two subbands, e_{g1} and e_{g2} separated by around 1.2 eV. The strong Hund's rule coupling further removes the spin degeneracy in the ferromagnetic regime giving rise to four subbands $e_{g1}\uparrow$, $e_{g1}\downarrow$, $e_{g2}\uparrow$, and $e_{g2}\downarrow$. The up and down subband are separated by an energy which is comparable ($\sim$1.5 eV) to the Jahn–Teller splitting energy. In the case of hole doped manganites such as $La_{1-x}Ca_xMnO_3$ or $La_{1-x}Sr_xMnO_3$ the lowest subband ($e_{g1}\uparrow$) band gets partially filled. Therefore the hole doped manganites are majority band ferromagnets (magnetization parallel to electron spin at Fermi energy). In the case of $La_{1-x}Ce_xMnO_3$ $e_{g1}\uparrow$ is full and it is not known whether the doped electrons get in the $e_{g1}\downarrow$ or $e_{g2}\uparrow$ subband. The system might correspondingly be a minority spin or a majority spin ferromagnet. It would be interesting to investigate this by a detailed study of the electronic band structure of $(LaCe)MnO_3$ to gain a more detailed understanding of the electronic properties of doped manganites and explore their application potentials.

IV. CONCLUSIONS

We have found that polycrystalline bulk samples of $La_{1-x}Ce_xMnO_3$ (x=0.025, 0.05, 0.1, 0.2, and 0.3) do not form in single phase, when synthesized by solid state reaction route. Phillip and Kutty tried to form these samples by wet-chemical method,[23] but their XRD patterns also contain extra peaks which are attribute as CeO_2 impurity peaks.

The partial phase formation,[21–23] which shows a metal insulator transition (though it can be clearly resolved into

two peaks) and a ferromagnetic ordering, supports the fact that cerium adopts a Ce^{4+} state in the lattice. Also we have been able to form the $La_{0.7}Ce_{0.3}MnO_3$ samples as both polycrystalline and epitaxial films in single phase by PLD, suggesting that it is the energetic laser ablation process which is responsible for the formation of these compounds (and not epitaxy unlike in $LuBa_2Cu_3O_7$). The laser ablated thin films not only show single phase nature when characterized by XRD, but also the unique and clean MIT peak accompanied by a sharp ferromagnetic transition corroborate the single phase nature of these films.

ACKNOWLEDGMENTS

We would like to thank Professor Chandrasekharan and S. P. Pai for rendering their assistance in XRD data analysis of the epitaxial films and in deposition of thin films, respectively.

[1] G. H. Jonker and J. H. Van Santen, Physica (Utrecht) **16**, 337 (1950).
[2] J. E. O. Wollan and W. C. Koehler, Phys. Rev. **100**, 545 (1955).
[3] G. H. Jonker, Physica (Utrecht) **22**, 707 (1956).
[4] C. Zener, Phys. Rev. **82**, 403 (1951); P. G. de Gennes, *ibid.* **118**, 141 (1960).
[5] A. Urushibara, Y. Morimoto, T. Arima, A. Asamitsu, G. Kido, and Y. Tokura, Phys. Rev. B **51**, 14103 (1995).
[6] M. McCormack, S. Jin, T. H. Teifel, R. M. Fleming, J. M. Phillips, and R. Ramesh, Appl. Phys. Lett. **64**, 3045 (1994).
[7] S. Jin, H. M. O'Bryan, T. H. Tiefel, M. McCormack, and W. W. Rhodes, Appl. Phys. Lett. **66**, 382 (1995).
[8] J. Z. Liu, I. C. Chang, S. Irons, P. Klavins, R. N. Shelton, K. Song, and S. R. Wasserman, Appl. Phys. Lett. **66**, 3218 (1995).
[9] H. L. Ju, J. Gopalakrishnan, J. L. Peng, Q. Li, G. C. Xiong, T. Venkateshan, and R. L. Greene, Phys. Rev. B **51**, 6143 (1995).
[10] V. Caignart, A. Maignan, and B. Raveau, Solid State Commun. **95**, 357 (1995).
[11] H. Y. Hwang, S. W. Cheong, P. G. Radaelli, M. Marezio, and B. Batlogg, Phys. Rev. Lett. **75**, 914 (1995).
[12] B. Raveau, A. Maignan, and V. Caignart, J. Solid State Chem. **117**, 424 (1995).
[13] J. M. De Teresa, J. Blasco, M. R. Ibara, J. Garcia, C. Marquina, P. A. AlgabareI, and A. del Moral, Solid State Commun. **96**, 627 (1995).
[14] Y. Tomioka, A. Asamitsu, Y. Morimoto, H. Kuwahara, and Y. Tokura, Phys. Rev. Lett. **74**, 5108 (1995).
[15] H. Y. Hwang, S. W. Cheong, P. G. Radaelli, M. Marezio, and B. Batlogg, Phys. Rev. Lett. **75**, 914 (1995).
[16] J. M. De Teresa, M. R. Ibara, J. Garcia, J. Blasco, C. Ritter, P. A. Algabarel, C. Marquina, and A. del Moral, Phys. Rev. Lett. **76**, 3392 (1996).
[17] J. B. Goodenough, Prog. Solid State Chem. **5**, 145 (1971).
[18] A. J. Millis, P. B. Littlewood, and B. I. Shraiman, Phys. Rev. Lett. **74**, 5144 (1995).
[19] P. Raychaudhuri, C. Mitra, A. Paramekanti, R. Pinto, A. K. Nigam, and S. K. Dhar, J. Phys.: Condens. Matter **10**, L191 (1998).
[20] P. Raychaudhuri, C. Mitra, A. K. Nigam, S. K. Dhar, and R. Pinto, Physica B **259**, 835 (1999).
[21] P. Mandal and S. Das, Phys. Rev. B **56**, 15073 (1997).
[22] J. R. Gebhardt, S. Roy, and N. Ali, J. Appl. Phys. **85**, 5390 (1999).
[23] J. Phillip and T. R. N. Kutty, J. Phys.: Condens. Matter **11**, 8537 (1999).
[24] H. M. Rietveld, Acta Crystallogr. **22**, 151 (1967).
[25] R. A. Young and D. B. Wiles, J. Appl. Crystallogr. **14**, 149 (1981).
[26] P. Raychaudhuri, S. Mukherjee, A. K. Nigam, J. John, U. D. Vaishnav, R. Pinto, and P. Mandal, J. Appl. Phys. **86**, 5718 (1999).
[27] K. I. Gnanasekar, M. Sharon, R. Pinto, S. P. Pai, M. S. R. Rao, P. R. Apte, A. S. Tamhane, S. C. Purandare, L. C. Gupta, and R. Vijayaraghavan, J. Appl. Phys. **79**, 1082 (1996).
[28] A. deAndres, M. Garcia-Hernandez, and J. L. Martinez, Phys. Rev. B **60**, 7328 (1999).